

Reaction of iron dicarbonyl phosphine complexes of 2-(phenylazo)pyridines with dimethyl acetylenedicarboxylate. Synthesis and crystal structure of a 2,3,1-diazaferrole complex

Martin N. Ackermann^{a,*}, Frederic V. Mikulec^a, Adam J. Matzger^a, Barbara J. Antonio^a,
M. Christopher Barron^a, Melissa J. Todd^a, Kathleen Meeker^a, Angeline L. Chupa^a,
Clifton Woods^b

^a Department of Chemistry, Oberlin College, Oberlin, OH 44074, USA

^b Department of Chemistry, University of Tennessee, Knoxville, TN 37996-1600, USA

Received 28 November 1995; in revised form 19 January 1996

Abstract

The complexes $\text{Fe}(\text{CO})_2(\text{P}^n\text{Bu}_3)\text{L}$ ($\text{L} = 2$ -(phenylazo)pyridine, 4-methyl-2-(phenylazo)pyridine, and 4,6-(dimethyl)-2-(phenylazo)pyridine) undergo a [3 + 2] cycloaddition reaction with dimethyl acetylenedicarboxylate (DMAD), $\text{RC}\equiv\text{CR}'$ ($\text{R} = \text{R}' = \text{COOCH}_3$), to produce the complexes $\text{Fe}(\text{CO})_2(\text{P}^n\text{Bu}_3)\text{C}(\text{COOCH}_3)=\text{C}(\text{COOCH}_3)\text{N}(\text{X-py})\text{N}(\text{Ph})$ ($\text{X} = \text{H}, 4\text{-CH}_3, 4,6\text{-(CH}_3)_2$), which contain a 2,3,1-diazaferrole ring. This reaction is very sensitive to the acetylene used and to the electron density at the iron center. No reaction occurs with an acetylene unless R and R' are both ester groups, and DMAD does not react with $\text{Fe}(\text{CO})_2(\text{P}^n\text{Bu}_3)$ (5-(trifluoromethyl)-2-(phenylazo)pyridine) or with the tricarbonyls $\text{Fe}(\text{CO})_3\text{L}$. The complexes $\text{Fe}(\text{CO})_2(\text{PPh}_3)\text{L}$ do not react with DMAD, presumably due to steric effects, but $\text{Fe}(\text{CO})_2(\text{P}(\text{OCH}_3)_3)(4\text{-methyl-2-phenylazopyridine})$ reacts to give $\text{Fe}(\text{CO})_2(\text{P}(\text{OCH}_3)_3)\text{C}(\text{COOCH}_3)=\text{C}(\text{COOCH}_3)\text{N}(4\text{-CH}_3\text{-2-py})\text{N}(\text{Ph})$. This complex crystallizes in the space group $P2_1/c$ with $a = 15.027(4)$ Å, $b = 8.244(1)$ Å, $c = 22.560(5)$ Å, $\beta = 108.03(2)^\circ$, $V = 2651.1(10)$ Å³ and $Z = 4$. The iron atom is in an approximate square pyramidal environment with $\text{P}(\text{OCH}_3)_3$ in the axial position. The 2,3,1-diazaferrole ring is essentially planar with sp^2 hybridization for all C and N ring atoms, and bond length data are consistent with a possible delocalized π system. The results obtained in this study are compared with similar studies on analogous α -diimine complexes.

Keywords: Iron; Phosphines; Acetylenes; Metalloacycles; π -Bonding

1. Introduction

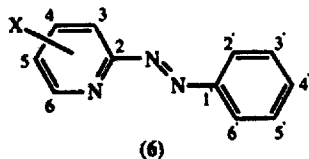
Coordinated α -diimines (1,4-diaza-1,3-diene, $\text{N}=\text{C}-\text{C}=\text{N}$) in complexes of the type $\text{M}(\alpha\text{-diimine})(\text{CO})_3$ ($\text{M} = \text{Fe}, \text{Ru}$) are activated towards a C–C coupling reaction with electron-deficient alkynes [1,2]. Although the initial bicyclo[2.2.1] adduct has not been isolated, considerable evidence indicates that this reaction proceeds by a 1,3-dipolar [3 + 2] cycloaddition followed by a sequence of rearrangement reactions according to Scheme 1 [1]. More recently, the isocyanide complexes $\text{M}(\alpha\text{-diimine})(\text{CO})_{3-n}(\text{CNR})_n$ ($\text{M} = \text{Fe}, \text{Ru}; n = 1$ and

3) have been found to undergo a similar reaction as well as addition to the $\text{Fe}-\text{C}=\text{N}$ fragment of the isocyanide [3–5]. Collectively, these studies reveal that the type and stability of products formed is highly sensitive to the electronic character of the metal center, as affected by the identity of both the metal and the ligands.

Recently we have been investigating the reaction of 2-(phenylazo)pyridines (6) with zero valent metal carbonyls with an interest, inter alia, in comparing the chemistry of this α -azoimine (1,2,4-triaza-1,3-diene, $\text{N}=\text{N}-\text{C}=\text{N}$) as a ligand to that of the more common and much studied α -diimines [6,7]. The poorer σ -donor and better π -acceptor abilities of the 2-(phenylazo)pyridines compared with α -diimines lead to significant differences in the properties of their complexes. Accord-

* Corresponding author.

ingly, we have extended our studies to the reaction of complexes of the type $\text{Fe}(\text{L-L}')(\text{CO})_2\text{L}''$ ($\text{L-L}' = \mathbf{6a-d}$; $\text{L}'' = \text{CO}, \text{PR}_3, \text{P}(\text{OR})_3$) with dimethyl acetylenedicarboxylate (DMAD), and herein report the results.



a, X = H; **b**, X = 4-CH₃; **c**, X = 4,6-(CH₃)₂; **d**, X = 5-CF₃

2. Experimental details

2.1. General procedures

All reactions were carried out under a dry and oxygen-free nitrogen atmosphere using standard Schlenk techniques or a drybox. Microanalyses were performed by Atlantic Microlab, Norcross, GA. Infrared spectra were recorded on a Perkin-Elmer Model 1760 FTIR at 1 cm⁻¹ resolution. UV-vis spectra were recorded on a Hewlett-Packard 8452 diode array spectrophotometer. Melting points were taken on a K fler hot-stage microscope and are uncorrected. ¹H and ¹³C NMR spectra were obtained on an IBM/Bruker NR200 instrument at 200 and 50.3 MHz respectively. Generally, NMR spectra of organometallic complexes were run in sealed tubes prepared on a vacuum line with CDCl₃ or CD₂Cl₂ that had been dried over P₄O₁₀ and degassed by several

freeze/thaw cycles. Chromatography columns were prepared by slurry-packing the stationary phase in petroleum ether.

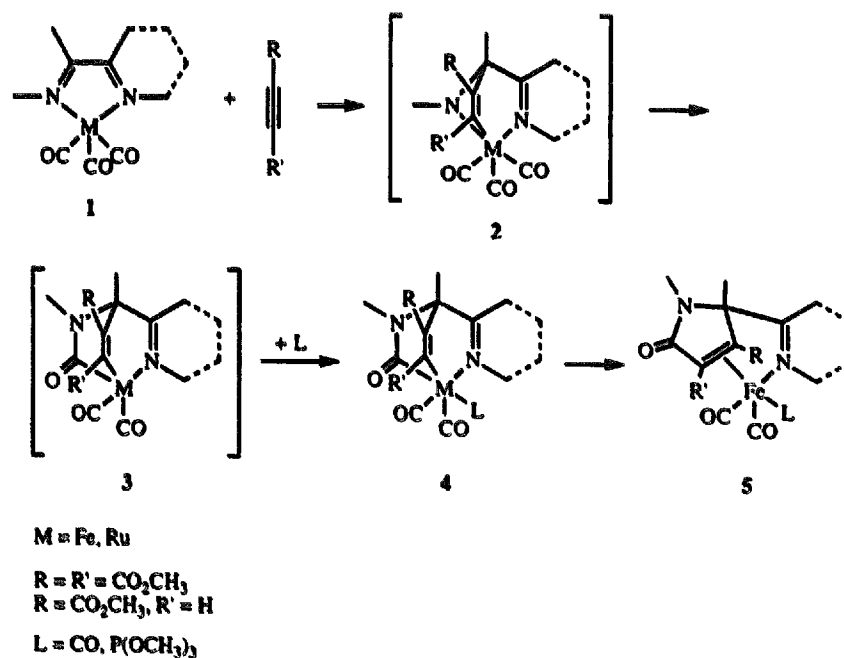
2.2. Materials and apparatus

Solvents were purified by distillation under nitrogen from a suitable drying agent. Hexanes was distilled from CaH₂, dichloromethane from P₄O₁₀, and tetrahydrofuran (THF) from sodium benzophenone ketyl.

Unless otherwise stated, chemicals were obtained from commercial sources and used as received. Trimethylphosphite was distilled from sodium under nitrogen. Dimethyl acetylenedicarboxylate (DMAD) and diethyl acetylenedicarboxylate (DEAD) were distilled under vacuum. The ligands 2-(phenylazo)pyridine (**6a**, 2-PAP), 4-methyl-2-(phenylazo)pyridine (**6b**, 4-CH₃-2-PAP), and 5-(trifluoromethyl)-2-(phenylazo)pyridine (**6d**, 5-CF₃-2-PAP), the iron tricarbonyl complexes Fe(CO)₃(2-PAP) (**7a**), Fe(CO)₃(4-CH₃-2-PAP) (**7b**), and Fe(CO)₃(5-CF₃-2-PAP) (**7d**), and the triphenylphosphine complexes Fe(CO)₂(2-PAP)(PPh₃), Fe(CO)₂(4-CH₃-2-PAP)(PPh₃), and Fe(CO)₂(5-CF₃-2-PAP)(PPh₃) were synthesized as previously described [7].

2.3. Synthesis of 4,6-(dimethyl)-2-(phenylazopyridine (4,6-diMe-2-PAP) (**6c**)

The synthesis of 4,6-diMe-2-PAP generally followed that described for 2-PAP, using 7.2 g of 4,6-dimethyl-2-pyridinamine and 6.6 g of nitrosobenzene as reactants [7]. However, the reaction mixture was heated at 110–115 °C for 20 min before cooling and work up. Chro-



Scheme 1.

matography of the crude product on an alumina column ($2 \times 40 \text{ cm}^2$) was accomplished using petroleum ether/ CH_2Cl_2 as eluant. The red–orange oil that remained after removing the solvent from the main orange band was recrystallized from petroleum ether. The yield was 4.6 g (22 mmol, 37%), m.p. 28–30 °C. Anal. Found: C, 48.11; H, 4.62; N, 7.24. $\text{C}_{13}\text{H}_{13}\text{N}_3$ Calc.: C, 48.02; H, 4.56; N, 7.30%. $^1\text{H NMR}$ (CDCl_3 , δ): 8.0–8.1 (m, 2H, H2' and H6'), 7.5–7.6 (m, 3H, H3', H4', and H5'), 7.40 (s, 1H, H3), 7.09 (s, 1H, H5), 2.64 (s, 3H, CH_3 at C6), 2.41 (s, 3H, CH_3 at C4). $^{13}\text{C}\{^1\text{H}\}$ NMR (CDCl_3 , δ): 162.8 (C2), 158.2 (C6), 152.3 (C1'), 149.7 (C4), 131.8 (C4'), 128.9 (C3' and C5'), 125.7 (C3), 123.4 (C2' and C6'), 111.4 (C5), 24.1 (C(6) CH_3), 21.0 (C(4) CH_3).

2.4. Synthesis of $\text{Fe}(\text{CO})_2(4,6\text{-diMe-2-PAP})(7\text{c})$

A mixture of 2.47 g (6.78 mmol) of $\text{Fe}_2(\text{CO})_9$ and 1.48 g (6.98 mmol) of **6c** in 100 ml of THF was stirred for 48 h at room temperature, and then the solvent was removed in vacuo. The solid residue was extracted with hexanes, and the solution filtered through a column of Celite ($2 \times 5 \text{ cm}^2$). The filtrate volume was reduced in vacuo until solid appeared, and then cooled to -78°C . The liquid was removed from the crystals using a cannula, and the crystals were washed several times with cold hexanes. The crystals were dried under vacuum while they slowly warmed to room temperature. The solid contained some unreacted **6c** which was removed by sublimation (approximately $40^\circ\text{C}/0.01$ Torr) followed by another recrystallization. The yield of **7c** was 1.52 g (4.32 mmol, 64%), m.p. 67–70 °C. Anal. Found: C, 54.83; H, 3.78; N, 12.00. $\text{C}_{16}\text{H}_{13}\text{FeN}_3\text{O}_3$ Calc.: C, 54.73; H, 3.73; N, 11.97%. IR (hexane): $\nu(\text{CO})$ 2039, 1977, 1961 cm^{-1} . $^1\text{H NMR}$ (CDCl_3 , δ): 7.83 (s, 1H, H3), 7.5–7.6 (m, 2H, H2' and H6'), 7.3–7.5 (m, 3H, H3', H4', and H5'), 6.76 (s, 1H, H5), 2.97 (s, 3H, CH_3 at C4), 2.42 (s, 3H, CH_3 at C6). $^{13}\text{C}\{^1\text{H}\}$ NMR (CDCl_3 , δ): 210.7 (CO), 163.4 and 161.7 (C2 and C1'), 156.9 (C6), 145.0 (C4), 128.4 (C3' and C5'), 127.4 (C4'), 123.7 (C2' and C6'), 119.1 and 118.3 (C3 and C5), 28.2 (C(6) CH_3), 20.6 (C(4) CH_3).

2.5. Synthesis of $\text{Fe}(\text{CO})_2(L-L)(P^{\text{n}}\text{Bu}_3)$ complexes (**8a–d**)

2.5.1. $\text{Fe}(\text{CO})_2(2\text{-PAP})(P^{\text{n}}\text{Bu}_3)$ (**8a**)

A mixture of 596 mg (1.84 mmol) of **7a** and 0.50 ml (2.1 mmol) of $P^{\text{n}}\text{Bu}_3$ was refluxed in 125 ml of hexanes until the infrared spectrum showed that the $\nu(\text{CO})$ bands of the starting complex had been replaced by bands of the product (around 24 h). The solvent and some of the excess $P^{\text{n}}\text{Bu}_3$ were removed in vacuo. The residue was taken up in hexanes, and the solution was filtered through a Celite column ($2 \times 5 \text{ cm}^2$). The filtrate volume was reduced under vacuum, and the solu-

tion was cooled to -78°C . After removal of the liquid using a cannula, the solid was washed several times with cold hexanes and then dried under vacuum while it warmed slowly to room temperature. Analytically pure **8a** was obtained after a second recrystallization which yielded 456 mg (0.92 mmol, 50%), m.p. 76–79 °C. Anal. Found: C, 60.22; H, 7.32; N, 8.42. $\text{C}_{25}\text{H}_{36}\text{FeN}_3\text{O}_2\text{P}$ Calc.: C, 60.37; H, 7.30; N, 8.45%. IR (hexane): $\nu(\text{CO})$ 1974, 1918 cm^{-1} . $^1\text{H NMR}$ (CDCl_3 , δ): 8.90 (d, 1H, H6), 7.78 (d, 1H, H3), 7.6–7.7 (m, 2H, H2' and H6'), 7.3–7.5 (m, 4H, H3', H5' H4', and H4), 6.69 (t, 1H, H5), 1.3–1.5 (m, 2H, PCH_2), 1.1–1.3 (m, 2H, PCH_2CH_2), 0.9–1.1 (m, 2H, $\text{PCH}_2\text{CH}_2\text{CH}_2$), 0.78 (t, 3H, $\text{PCH}_2\text{CH}_2\text{CH}_2\text{CH}_3$). $^{13}\text{C}\{^1\text{H}\}$ NMR (CDCl_3 , δ): 218.8 (d, $^2J_{\text{CP}} = 8.0$ Hz, CO), 161.0 (d, $^3J_{\text{CP}} = 4.0$ Hz, C1'), 159.7 (C2), 150.5 (C6), 130.2 (C4), 128.2 (C3' and C5'), 126.1 (C4'), 123.9 (C2' and C6'), 119.5 (C3), 111.8 (C5), 25.9 (d, $J_{\text{CP}} = 22.5$ Hz, PCH_2), ~ 24 (two doublets, $\text{PCH}_2\text{CH}_2\text{CH}_2\text{CH}_3$), 13.5 (d, $^4J_{\text{CP}} = 5.0$ Hz, $\text{PCH}_2\text{CH}_2\text{CH}_2\text{CH}_3$).

2.5.2. $\text{Fe}(\text{CO})_2(4\text{-CH}_3\text{-2-PAP})(P^{\text{n}}\text{Bu}_3)$ (**8b**)

The procedure was the same as that for **8a**. Use of 409 mg (1.21 mmol) of **7b** and 0.30 ml (1.22 mmol) of $P^{\text{n}}\text{Bu}_3$ gave 451 mg (0.88 mmol, 73%) of analytically pure **8b**, m.p. 90–91 °C after one crystallization. Anal. Found: C, 60.98; H, 7.50; N, 8.21. $\text{C}_{26}\text{H}_{38}\text{FeN}_3\text{O}_2\text{P}$ Calc.: C, 61.06; H, 7.49; N, 8.22%. IR (hexane): $\nu(\text{CO})$ 1971, 1915 cm^{-1} . $^1\text{H NMR}$ (CDCl_3 , δ): 8.74 (d, 1H, H6), 7.6–7.7 (m, 3H, H3, H2', and H6'), 7.3–7.4 (m, 3H, H3', H4', and H5'), 6.55 (dd, 1H, H5), 2.34 (s, CH_3 at C4), 1.3–1.5 (m, 2H, PCH_2), 1.1–1.3 (m, 2H, PCH_2CH_2), 0.9–1.1 (m, 2H, $\text{PCH}_2\text{CH}_2\text{CH}_2$), 0.78 (t, 3H, $\text{PCH}_2\text{CH}_2\text{CH}_2\text{CH}_3$). $^{13}\text{C}\{^1\text{H}\}$ NMR (CDCl_3 , δ): 219.0 (d, $^2J_{\text{CP}} = 7.5$ Hz, CO), 161.1 (d, $^3J_{\text{CP}} = 3$ Hz, C1'), 160.2 (C2), 149.7 (C6), 141.3 (C4), 128.1 (C3' and C5'), 126.0 (C4'), 123.9 (C2' and C6'), 118.5 (C3), 114.4 (C5), 25.9 (d, $J_{\text{CP}} = 22.0$ Hz, PCH_2), ~ 24 (two doublets, $\text{PCH}_2\text{CH}_2\text{CH}_2\text{CH}_3$), 20.8 (CH_3 at C4), 13.4 ($\text{PCH}_2\text{CH}_2\text{CH}_2\text{CH}_3$).

2.5.3. $\text{Fe}(\text{CO})_2(4,6\text{-diMe-2-PAP})(P^{\text{n}}\text{Bu}_3)$ (**8c**)

The procedure was the same as that for **8a**, using 930 mg (2.65 mmol) of **7c** and 0.68 ml (2.7 mmol) of $P^{\text{n}}\text{Bu}_3$. The yield of **8c** was 1.24 g (2.36 mmol, 89%), m.p. 119–120 °C. Anal. Found: C, 61.84; H, 7.72; N, 8.01. $\text{C}_{27}\text{H}_{40}\text{FeN}_3\text{O}_2\text{P}$ Calc.: C, 61.72; H, 7.67; N, 8.00%. IR (hexane): $\nu(\text{CO})$ 1968, 1910 cm^{-1} . $^1\text{H NMR}$ (CDCl_3 , δ): 7.64 (s, 1H, H3), 7.6–7.7 (m, 2H, H2' and H6'), 7.3–7.4 (m, 3H, H3', H4', and H5'), 6.58 (s, 1H, H5), 2.95 (s, CH_3 at C6), 2.34 (s, CH_3 at C4), 1.3–1.5 (m, 2H, PCH_2), 1.0–1.2 (m, 2H, PCH_2CH_2), 0.8–1.0 (m, 2H, $\text{PCH}_2\text{CH}_2\text{CH}_2$), 0.75 (t, 3H, $\text{PCH}_2\text{CH}_2\text{CH}_2\text{CH}_3$). $^{13}\text{C}\{^1\text{H}\}$ NMR (CDCl_3 , δ): 217.8 (d, $^2J_{\text{CP}} = 7.0$ Hz, CO), 161.5 (C2), 161.2 (d, $^3J_{\text{CP}} = 2.5$ Hz, C1'), 156.7 (C6), 141.9 (C4), 128.0 (C3' and C5'),

126.2 (C4'), 124.0 (C2' and C6'), 116.8 and 115.8 (C3 and C5), 29.5 (CH₃ at C6), 26.6 (d, $J_{CP} = 21.5$ Hz, PCH₂), ~ 24 (two doublets, PCH₂CH₂CH₂CH₃), 20.4 (CH₃ at C4), 13.3 (PCH₂CH₂CH₂CH₃).

2.5.4. $Fe(CO)_2(5-CF_3-2-PAP)(P^nBu_3)$ (**8d**)

The procedure was the same as that for **8a**, using 641 mg (1.64 mmol) of **7d** and 0.42 ml (1.7 mmol) of PⁿBu₃. A small amount of 5-CF₃-2-PAP was removed from the crystals by sublimation (approximately 40 °C/0.01 Torr). The yield of **8d** was 588 mg (1.04 mmol, 63%), m.p. 77–80 °C. Anal. Found: C, 55.04; H, 6.23; N, 7.37. C₂₆H₃₅F₃FeN₃O₂P Calc.: C, 55.23; H, 6.24; N, 7.43%. IR (hexane): $\nu(CO)$ 1982, 1928 cm⁻¹. ¹H NMR (CDCl₃, δ): 9.12 (qt, 1H, H6), 7.74 (d of qt, 1H, H4), 7.6–7.7 (m, 2H, H2' and H6'), 7.3–7.4 (m, 3H, H3', H4', and H5'), 1.3–1.5 (m, 2H, PCH₂), 1.1–1.3 (m, 2H, PCH₂CH₂), 0.9–1.1 (m, 2H, PCH₂CH₂CH₂), 0.79 (t, 3H, PCH₂CH₂CH₂CH₃). ¹³C{¹H} NMR (CDCl₃, δ): 217.5 (d, $^2J_{CP} = 9.5$ Hz, CO), 160.9 (d, $^3J_{CP} = 2.5$ Hz, C1'), 158.4 (C2), 148.5 (qt, $^3J_{CF} = 5.3$ Hz, C6), 128.3 (C3' and C5'), 126.6 (C4'), 125.7 (C4), 123.9 (C2' and C6'), 124.5 (qt, $^1J_{CF} = 271.5$ Hz, CF₃), 119.1 (C3), 114.4 (qt, $^2J_{CF} = 33.0$ Hz, C5), 26.0 (d, $J_{CP} = 23.0$ Hz, PCH₂), ~ 24 (two doublets, PCH₂CH₂CH₂CH₃), 13.3 (PCH₂CH₂CH₂CH₃).

2.6. Synthesis of $Fe(CO)_2(4-CH_3-2-PAP)(P(OCH_3)_3)$ (**9b**)

The procedure was similar to that for the synthesis of **8a**. A mixture of 605 mg (1.79 mmol) of **7b** and 0.22 ml (1.9 mmol) of P(OCH₃)₃ was refluxed in 50 ml of hexanes for 72 h. After recrystallization, some residual P(OCH₃)₃ was removed by sublimation (approximately 45 °C/0.01 Torr), leaving 459 mg (1.06 mmol, 59%) of **9b**, m.p. 75–77 °C. Anal. Found: C, 46.21; H, 4.73; N, 9.55. C₁₇H₂₀FeN₃O₃P Calc.: C, 47.14; H, 4.65; N, 9.70%. IR (hexane): $\nu(CO)$ 1993, 1939 cm⁻¹. ¹H NMR (CDCl₃, δ): 8.86 (d, 1H, H6), 7.6–7.7 (m, 3H, H3, H2', and H6'), 7.3–7.5 (m, 3H, H3', H4', and H5'), 6.58 (dd, 1H, H5), 2.36 (s, CH₃ at C4), 3.28 (d, $^3J_{CP} \approx 12.0$ Hz, OCH₃). ¹³C{¹H} NMR (CDCl₃, δ): 216.5 (d, $^2J_{CP} = 12.5$ Hz, CO), 161.0 (d, $^3J_{CP} \approx 5$ Hz, C1'), 160.6 (C2), 150.7 (C6), 142.3 (C4), 128.3 (C3' and C5'), 126.4 (C4'), 124.0 and 123.9 (C2' and C6'), 118.6 (C3), 114.8 (C5), 51.3 (d, $^2J_{CP} \approx 3$ Hz, OCH₃), 20.9 (CH₃ at C4).

2.7. Synthesis of $Fe(CO)_2(P^nBu_3)C(COOCH_3)=C(COOCH_3)N(X-2-py)N(Ph)$ complexes (**11a–c**)

2.7.1. $Fe(CO)_2(P^nBu_3)C(COOCH_3)=C(COOCH_3)N(2-py)N(Ph) \cdot 0.5CH_2Cl_2$ (**11a**)

A mixture of 782 mg (1.57 mmol) of **8a** and 0.20 ml (1.6 mmol) of DMAD in 125 ml of CH₂Cl₂ was stirred

at room temperature until the infrared spectrum showed that the carbonyl bands of the starting complex had been replaced by bands of the product (around 3 h), and then the solvent was removed in vacuo. The residue was dissolved in a minimum amount of CH₂Cl₂ and filtered through a Celite column (2 × 5 cm²). About three times the volume of hexanes was added to the filtrate, the volume of the resulting mixture was reduced until solid began to form, and the solution was cooled to –78 °C. The liquid was removed using a cannula, and the solid was washed several times with cold hexanes and then dried under vacuum while it warmed slowly to room temperature. A second recrystallization gave 406 mg (0.59 mmol, 38%) of **11a**, m.p. 160–162 °C. Anal. Found: C, 55.35; H, 6.30; N, 6.17. C_{31.5}H₄₃ClFeN₃O₆P Calc.: C, 55.48; H, 6.36; N, 6.16%. IR (hexane): $\nu(CO)$ 1986, 1932 cm⁻¹. ¹H NMR (CDCl₃, δ): 8.27 (dm, 1H, H6), 7.36 (td, 1H, H4), 7.0–7.2 (m, 5H, H2', H3', H4', H5', and H6'), 7.00 (ddd, 1H, H5), 6.75 (d, 1H, H3), 3.86 (s, 3H, OCH₃), 3.58 (s, 3H, OCH₃), 1.5–1.7 (m, 2H, PCH₂), 1.2–1.4 (m, 2H, PCH₂CH₂), 1.0–1.2 (m, 2H, PCH₂CH₂CH₂), 0.85 (t, 3H, PCH₂CH₂CH₂CH₃). ¹³C{¹H} NMR (CDCl₃, δ): 215.6 (d, $^2J_{CP} = 16.0$ Hz, Fe–CO), 177.7 (Fe–C–CO₂CH₃), 173.1 (d, $^2J_{CP} = 17.5$ Hz, Fe–C=C), 162.2 (Fe–C=C–CO₂CH₃), 155.1 (C1'), 153.5 (C2), 147.9 (C6), 141.1 (Fe–C=C–N), 136.5 (C4), 127.5 (C3' and C5'), 126.3/125.6 (C2', C4', and C6'), 122.5 (C3 and C5), 51.9/51.2 (Fe–C(CO₂CH₃)=C(CO₂CH₃), 28.2 (d, $J_{CP} = 25.5$ Hz, PCH₂), 24–25 (two doublets, PCH₂CH₂CH₂CH₃), 13.5 (d, PCH₂CH₂CH₂CH₃).

2.7.2. $Fe(CO)_2(P^nBu_3)C(COOCH_3)=C(COOCH_3)N(4-CH_3-2-py)N(Ph)$ (**11b**)

The procedure followed that for **11a** but with THF as the solvent. The reaction of 556 mg (1.09 mmol) of **8b** and 0.40 ml (3.3 mmol) of DMAD was over in 46 h. Two recrystallizations from hexanes gave 512 mg (0.88 mmol, 79%) of **11b**, m.p. 135–139 °C. Anal. Found: C, 58.86; H, 6.80; N, 6.41. C₃₂H₄₄FeN₃O₆P Calc.: C, 58.81; H, 6.79; N, 6.43%. IR (hexane): $\nu(CO)$ 1985, 1931 cm⁻¹. ¹H NMR (CDCl₃, δ): 8.11 (dd, 1H, H6), 7.0–7.2 (m, 5H, H2', H3', H4', H5', and H6'), 6.81 (ddd, 1H, H5), 6.75 (d, 1H, H3), 3.85 (s, 3H, OCH₃), 3.60 (s, 3H, OCH₃), 2.07 (s, CH₃ at C4), 1.5–1.7 (m, 2H, PCH₂), 1.2–1.4 (m, 2H, PCH₂CH₂), 1.0–1.2 (m, 2H, PCH₂CH₂CH₂), 0.85 (t, 3H, PCH₂CH₂CH₂CH₃). ¹³C{¹H} NMR (CDCl₃, δ): 215.7 (d, $^2J_{CP} = 16.0$ Hz, Fe–CO), 177.6 (Fe–C–CO₂CH₃), 172.8 (d, $^2J_{CP} = 17.5$ Hz, Fe–C=C), 162.3 (Fe–C=C–CO₂CH₃), 155.2 (C1'), 153.5 (C2), 148.0 (C4), 147.4 (C6), 141.2 (Fe–C=C–N), 127.4 (C3' and C5'), 126.2/125.6 (C2', C4', and C6'), 123.4 (C3 and C5), 51.9/51.2 (Fe–C(CO₂CH₃)=C(CO₂CH₃), 28.3 (d, $J_{CP} = 25.0$ Hz, PCH₂), 24–25 (two doublets, PCH₂CH₂CH₂CH₃), 20.5 (CH₃ at C4), 13.5 (d, PCH₂CH₂CH₂CH₃).

2.7.3. $\text{Fe}(\text{CO})_2(\text{P}^n\text{Bu}_3)_2(\text{C}(\text{COOCH}_3))=\text{C}(\text{COOCH}_3)\text{N}(4,6\text{-diMe-2-py})\text{N}(\text{Ph})$ (**11c**)

The procedure was the same as that for **11a** except that the solid from crystallization was subjected to sublimation (approximately 45 °C/0.01 Torr) to remove residual DMAD and some **6c**. The reaction of 398 mg (0.757 mmol) of **6c** and 0.20 ml (1.6 mmol) of DMAD was complete in 10 h and provided 360 mg (0.544 mmol, 72%) of **11c**, m.p. 81–83 °C. Anal. Found: C, 59.23; H, 7.00; N, 6.19. $\text{C}_{33}\text{H}_{46}\text{FeN}_3\text{O}_6\text{P}$ Calc.: C, 59.38; H, 6.95; N, 6.29%. IR (hexane): $\nu(\text{CO})$ 1985, 1930 cm^{-1} . ^1H NMR (CDCl_3 , δ): 7.0–7.2 (m, 5H, H2', H3', H4', H5', and H6'), 6.66 (s, 1H, H5), 6.32 (s, 1H, H3), 3.84 (s, 3H, OCH_3), 3.60 (s, 3H, OCH_3), 2.30 (s, CH_3 at C6), 2.01 (s, CH_3 at C4), 1.6–1.8 (m, 2H, PCH_2), 1.2–1.4 (m, 2H, PCH_2CH_2), 1.0–1.2 (m, 2H, $\text{PCH}_2\text{CH}_2\text{CH}_2$), 0.85 (t, 3H, $\text{PCH}_2\text{CH}_2\text{CH}_2\text{CH}_3$). $^{13}\text{C}\{^1\text{H}\}$ NMR (CDCl_3 , δ): 215.8 (d, $^2J_{\text{CP}} = 15.5$ Hz, Fe–CO), 177.6 (Fe–C– CO_2CH_3), 171.8 (d, $^2J_{\text{CP}} = 18.0$ Hz, Fe–C=C), 162.8 (Fe–C=C– CO_2CH_3), 156.5 (C6), 155.2 (C1'), 152.4 (C2), 148.0 (C4), 141.6 (Fe–C=C–N), 127.3 (C3' and C5'), 126.2/125.5 (C2', C4', and C6'), 122.7/120.1 (C3 and C5), 51.8/51.2 (Fe–C(CO_2CH_3)=C(CO_2CH_3)), 28.3 (d, $J_{\text{CP}} = 25.0$ Hz, PCH_2), 23.6 (CH_3 at C6), 20.4 (CH_3 at C4), 24–25 (two doublets, $\text{PCH}_2\text{CH}_2\text{CH}_2\text{CH}_3$), 13.5 (d, $\text{PCH}_2\text{CH}_2\text{CH}_2\text{CH}_3$).

2.8. Synthesis of $\text{Fe}(\text{CO})_2(\text{P}(\text{OCH}_3)_3)_2(\text{C}(\text{COOCH}_3))=\text{C}(\text{COOCH}_3)\text{N}(4\text{-CH}_3\text{-2-py})\text{N}(\text{Ph})$ (**12b**)

The procedure was similar to that for **11b**. The reaction of 303 mg (0.700 mmol) of **9b** and 0.30 ml (2.4 mmol) of DMAD was over in 24 h. One recrystallization gave 243 mg (0.42 mmol, 60%) of **12b**, m.p. 135–138 °C. The result was comparable when CH_2Cl_2 was used as the reaction solvent. Anal. Found: C, 48.11; H, 4.62; N, 7.10. $\text{C}_{23}\text{H}_{26}\text{FeN}_3\text{O}_9\text{P}$ Calc.: C, 48.02; H, 4.53; N, 7.30%. IR (CH_2Cl_2): $\nu(\text{CO})$ 2005, 1950 cm^{-1} . ^1H NMR (CDCl_3 , δ): 8.10 (d, 1H, H6), 7.0–7.2 (m, 5H, H2', H3', H4', H5', and H6'), 6.84 (d, 1H, H5), 6.60 (s, 1H, H3), 3.86 (s, 3H, COCH_3), 3.61 (s, 3H, COCH_3), 2.16 (s, CH_3 at C4), 3.44 (d, $^3J_{\text{HP}} \cong 12.2$ Hz, POCH_3). $^{13}\text{C}\{^1\text{H}\}$ NMR (CDCl_3 , δ): 212.8 (d, $^2J_{\text{CP}} = 23.5$ Hz, Fe–CO), 176.8 (Fe–C– CO_2CH_3), 172.9 (d, $^2J_{\text{CP}} = 22.0$ Hz, Fe–C=C), 161.8 (Fe–C=C– CO_2CH_3), 154.7 (C1'), 152.9 (C2), 148.3 (C4), 147.7 (C6), 140.6 (Fe–C=C–N), 127.4 (C3' and C5'), 126.6/126.2 (C2', C4', and C6'), 124.0/123.7 (C3 and C5), 52.2/51.4 (Fe–C(CO_2CH_3)=C(CO_2CH_3)), 51.9 (d, $^2J_{\text{CP}} = 3.5$ Hz, POCH_3), 20.5 (CH_3 at C4).

2.9. Synthesis of $\text{Fe}(\text{CO})_2(\text{P}(\text{OCH}_3)_3)_2(\text{C}(\text{COOCH}_2\text{CH}_3))=\text{C}(\text{COOCH}_2\text{CH}_3)\text{N}(4\text{-CH}_3\text{-2-py})\text{N}(\text{Ph})$

The procedure was similar to that for **12b** except CH_2Cl_2 was the solvent. The reaction of 272 mg (0.627 mmol) of **9b** and 0.14 ml (0.875 mmol) of DEAD was

complete in 15 h. However, repeated recrystallizations and sublimations of the tacky solid failed to yield a pure material. IR (CH_2Cl_2): $\nu(\text{CO})$ 2003, 1948 cm^{-1} .

2.10. Reaction of **8a–c** and **9b** with DMAD in the presence of CO

The reaction was run and worked up as for the synthesis of **11a–c** or **12b** except an atmosphere of CO was maintained above the reaction solution. The reaction was monitored until the infrared spectrum showed that the $\nu(\text{CO})$ bands of the starting complex were gone. New bands appeared at 2057 and 1980 cm^{-1} with a shoulder at about 1990 cm^{-1} in THF and at 2061 and 1984 cm^{-1} with a shoulder at about 1995 cm^{-1} in CH_2Cl_2 and were independent of the starting complex within 1 cm^{-1} . After removal of solvent, the residue was dissolved in a few milliliters of CH_2Cl_2 and then a large volume of hexanes was added to precipitate non-carbonyl containing material. The solution was filtered through a short column of Celite, the volume of the filtrate was reduced, and the solution was cooled to –78 °C. The liquid was removed using a cannula, and the oily residue was washed several times with cold hexanes and then dried under vacuum while it warmed slowly to room temperature. Several recrystallizations failed to yield a pure material as judged by NMR. Chromatography on Florisil ($2 \times 50 \text{ cm}^2$) at 0 °C using up to 30% THF in petroleum ether gave a trace of a pink band followed by an orange band. Removal of solvent left a small amount of orange solid that showed little improvement in purity compared with the initial material.

2.11. Reaction of **11a–c** and **12b** with CO

About 0.05 mmol of **11a–c** or **12b** was dissolved in 25 ml of THF or CH_2Cl_2 and an atmosphere of CO was introduced. Infrared monitoring in the carbonyl stretching region showed no changes over several days.

2.12. Reaction of **11a–c** and **12b** with CO in the presence of DMAD

About 0.05 mmol of **11a–c** or **12b** was dissolved in 25 ml of THF or CH_2Cl_2 and 0.1 to 3 times the equivalent amount of DMAD was added. An atmosphere of CO was introduced and the infrared spectrum was monitored in the carbonyl stretching region. The same new bands grew as described in Section 2.9. Loss of starting complex was complete in about a week when 1–3 equivalents of DMAD were initially present, but the conversion was far from complete in the same period for 0.1 equivalent of DMAD.

2.13. X-ray structure determination of **12b**

Crystals were obtained by vapor diffusion of pentane into a solution of **12b** in toluene. A red crystal of **12b**

Table 1
Crystallographic data for 12b

Formula	C ₂₃ H ₂₆ FeN ₃ O ₃ P
FW	575.3
Crystal system	Monoclinic
Space group	P2 ₁ /c
Z	4
a (Å)	15.027(4)
b (Å)	8.224(1)
c (Å)	22.560(5)
β (deg)	108.03(2)
V (Å ³)	2651.1(10)
d(calc) (g cm ⁻³)	1.441
λ(Mo Kα) (Å)	0.71073
μ (cm ⁻¹)	6.8
No. of observed reflections	2512 (F > 4.0σ(F))
R, R _w ^a	0.0789, 0.1131

$$^a R = [\sum \|F_o\| - |F_c|] / [\sum \|F_o\|]; R_w = [\sum w(|F_o| - |F_c|)^2]^{1/2} / [\sum wF_o^2] \text{ where } w = [\sigma^2(F_o) + 0.0036F_o^2]^{-1/2}.$$

with dimensions 0.2 × 0.4 × 0.45 mm³ was used for the structure determination. The crystallographic data were collected on a Siemens R3mV diffractometer equipped with a graphite monochromator. Unit cell dimensions and a crystal orientation matrix were obtained by least-squares refinement of the diffractometer setting angles of a group of high angle reflections. Data were collected by the ω scan method. The intensities of three standard reflections were monitored every 97 reflections and exhibited no significant variation during the data collection. The data were corrected for Lorentz and polarization effects. The absorption coefficient was 6.8 cm⁻¹. The structure was solved by direct methods and successive Fourier difference procedures [8,9]. During the final stages of full-matrix least-squares refinement hydrogen atoms were included at their calculated positions (*d*_{C-H} = 0.96 Å). Although the hydrogen atoms were not refined, they were allowed to ride along with their bonded carbon atoms during the refinement. The final

Table 2
Selected bond distances (Å) and angles (deg) for 12b

Fe-P	2.131(2)	Fe-N(1)	1.853(8)
Fe-C(1)	1.767(12)	Fe-C(2)	1.784(10)
Fe-C(8)	1.938(9)	N(1)-N(2)	1.374(11)
N(2)-C(9)	1.382(12)	O(1)-C(1)	1.144(14)
O(2)-C(2)	1.139(13)	C(8)-C(9)	1.367(14)
P-Fe-N(1)	116.9(2)	P-Fe-C(1)	98.0(3)
N(1)-Fe-C(1)	144.9(4)	P-Fe-C(2)	92.5(3)
N(1)-Fe-C(2)	92.6(4)	C(1)-Fe-C(2)	89.9(5)
P-Fe-C(8)	95.8(3)	N(1)-Fe-C(8)	82.0(4)
C(1)-Fe-C(8)	90.8(4)	C(2)-Fe-C(8)	171.5(4)
Fe-N(1)-N(2)	117.1(6)	Fe-N(1)-C(12)	129.7(6)
N(2)-N(1)-C(12)	112.5(8)	N(1)-N(2)-C(9)	112.6(8)
N(1)-N(2)-C(18)	122.2(8)	C(9)-N(2)-C(18)	123.3(8)
Fe-C(8)-C(9)	113.2(7)	N(2)-C(9)-C(8)	114.9(8)
N(2)-C(9)-C(10)	116.7(9)	C(8)-C(9)-C(10)	128.2(8)

Table 3
Atomic coordinates (× 10⁴) and equivalent isotropic displacement coefficients (Å² × 10³) for 12b

Atom	x	y	z	U _{eq} ^a
Fe	1823(1)	1635(2)	1733(1)	22(1)
P	619(2)	111(3)	1449(1)	23(1)
N(1)	2408(5)	2095(9)	1140(3)	21(3)
N(2)	3100(5)	1046(10)	1101(3)	27(3)
N(3)	4528(7)	2085(4)	1085(7)	85(6)
O(1)	1944(6)	2086(10)	3034(4)	59(4)
O(2)	702(5)	4606(10)	1475(3)	48(3)
O(3)	561(5)	-1527(8)	1812(3)	37(3)
O(4)	-323(4)	1049(8)	1409(3)	27(2)
O(5)	359(4)	-597(8)	756(3)	33(2)
O(6)	2852(4)	-2922(8)	2152(3)	33(3)
O(7)	2918(6)	-1213(10)	2937(3)	52(3)
O(8)	4592(4)	-1568(8)	2132(3)	33(3)
O(9)	4110(5)	-2015(8)	1103(3)	40(3)
C(1)	1899(6)	1824(12)	2528(5)	33(4)
C(2)	1135(7)	3442(13)	1561(4)	32(4)
C(3)	562(8)	-1517(15)	2447(5)	53(5)
C(4)	-1221(7)	282(13)	1182(5)	40(4)
C(5)	998(7)	-1652(14)	582(5)	42(4)
C(6)	3063(8)	-4226(13)	2601(5)	50(5)
C(7)	2868(6)	-1413(12)	2396(4)	25(3)
C(8)	2728(6)	-121(11)	1930(4)	23(3)
C(9)	3292(6)	-142(11)	1557(4)	24(3)
C(10)	4028(6)	-1345(11)	1550(5)	26(3)
C(11)	5291(8)	-2851(14)	2217(6)	51(5)
C(12)	2163(6)	3241(11)	643(4)	24(3)
C(13)	1412(6)	2911(12)	122(4)	31(4)
C(14)	1182(8)	3982(14)	-374(5)	46(4)
C(15)	1688(7)	5416(13)	-342(5)	41(4)
C(16)	2423(7)	5786(12)	187(4)	31(4)
C(17)	2669(7)	4685(12)	684(5)	32(4)
C(18)	3714(7)	1413(14)	733(6)	49(5)
C(19)	3372(10)	1120(19)	113(5)	80(7)
C(20)	4162(15)	1803(25)	-175(6)	107(9)
C(21)	3836(15)	1792(45)	-753(14)	293(28)
C(22)	4957(10)	2471(21)	254(7)	75(7)
C(23)	5130(13)	2539(24)	818(10)	108(10)

^a Equivalent isotropic *U* defined as one third of the trace of the orthogonalized *U*_{*i*} tensor.

difference map contained several residual electron density peaks in the vicinity of the 4-methylpyridyl ring, that suggested the pyridyl group was disordered as a result of rotation about the N(2)-C(18) bond. Indeed, the largest shift/esds during the final refinement were for thermal parameters of C(20) and C(21). Attempts to model the disorder to improve the structure determination were not successful.

A summary of crystal data is given in Table 1. A complete set of crystal, collection, and solution and refinement data can be found in the supplementary material. Selected bond distances and angles for 12b are listed in Table 2, and atomic coordinates and isotropic thermal parameters for the non-hydrogen atoms in Table 3.

3. Results and discussion

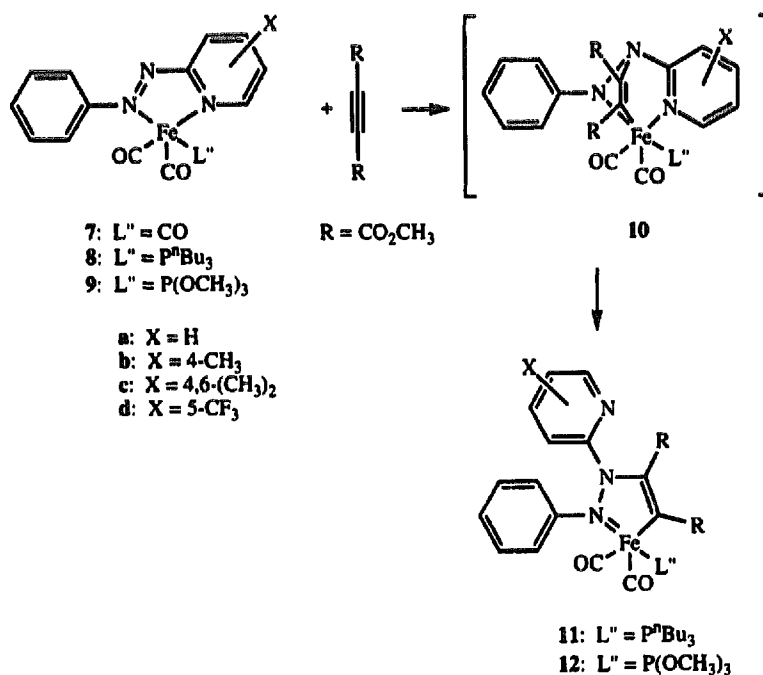
3.1. Syntheses

Unlike the α -diimine iron tricarbonyl complexes **1** ($M = \text{Fe}$), the PAP tricarbonyl complexes **7a–d** do not react with the activated acetylene DMAD. However, when one of the carbonyl groups is replaced by a P^nBu_3 group, the complexes **8a–c**, but not **8d**, react with DMAD at room temperature to form compounds of type **11**, a 2,3,1-diazaferrole, whose structure has been confirmed by an X-ray crystallography study of the related compound **12b** (vide infra). In contrast, the analogous triphenylphosphine complexes $\text{Fe}(\text{CO})_2(\text{L}-\text{L}')(\text{PPh}_3)$ ($\text{L}-\text{L}' = \mathbf{6a-d}$) do not react with DMAD. Initially, reactions were run in THF, but only **8b** reacted cleanly to give **11b**. **8a** and **8c** gave a mixture from which a pure product (**11a** or **11c**) could not be obtained by crystallization, and chromatography on Florisil resulted in decomposition. Subsequently, **11a** and **11c** were obtained using CH_2Cl_2 as solvent, in which the reactions are faster (hours instead of days) and cleaner.

By analogy with the α -diimine complexes **1** (Scheme 1), we propose that the first step in the reaction sequence leading to **11** is a 1,3-dipolar addition reaction to give **10**, analogous to **2** (Scheme 2). Like **2**, **10** has not been observed. One possibility is that the intermediate **10** never forms because the breaking of the iron–pyridyl bond occurs simultaneously with the [3 + 2] cycloaddition. Another possibility is that **10** is formed

but is too short-lived to be observed. We note also the absence of a carbonyl insertion product, such as **4**, in the PAP system. Obviously, this reaction cannot occur if **10** is never formed. However, such reactions normally occur by a migratory insertion mechanism [10], and reaction may not be favorable because the nitrogen atom in the PAP case is not sufficiently nucleophilic due to the presence of the additional nitrogen instead of a carbon atom.

Cycloaddition reactions are known to be sensitive to the energies of the interacting frontier orbitals [2,3]. The failure of the PAP tricarbonyl complexes **7** to react with DMAD must be due to the reduced electron density at the iron center because of the poorer σ -donor and better π -acceptor abilities of the 2-(phenylazo)pyridines compared with α -diimines. Since phosphines are better σ -donating and poorer π -accepting ligands than CO, they increase the electron density on iron in **8** such that the cycloaddition reaction occurs. Even so, the rate of reaction is quite slow compared with the iron and the even more electron-rich ruthenium α -diimine complexes [2]. The high sensitivity to electronic effects is illustrated by the fact that only complexes **8a–c** react. The reactivity order is **8b** > **8a** > **8c** in either THF or CH_2Cl_2 . We attribute **8b** > **8a** to the increased electron density at the iron resulting from replacing a hydrogen on the pyridyl ring with an electron-donating methyl group. On these grounds the two methyl groups in **8c** should result in an even faster rate. The lower reactivity for **8c** with two methyl groups is likely to be a conse-



Scheme 2.

quence of the steric effect from the methyl group *ortho* to the pyridyl nitrogen. In the case of **8d** the electron-withdrawing CF₃ substituent on the pyridyl ring apparently lowers the electron density at the iron far enough to preclude reaction.

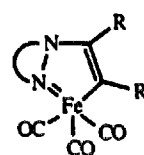
The trimethylphosphite complex Fe(CO)₂(4-CH₃-2-PAP)(P(OCH₃)₃) (**9b**) also reacts readily with DMAD to give **12b**. Since the donor ability increases in the order P(OCH₃)₃ < PPh₃ < PⁿBu₃, while cone angles increase in the order P(OCH₃)₃ < PⁿBu₃ < PPh₃ [11,12], the lack of reaction in the case of the triphenylphosphine complexes Fe(CO)₂(L-L')(PPh₃) (L-L' = **6a-d**) must be due to steric factors. Related steric effects have been observed with diimine complexes; when (Scheme 1) L = PPh₃, the conversion of **2** to **4** occurs in the case of M = Ru but not when M is the smaller Fe atom [2].

The iron α -diimine tricarbonyl complex **1** also reacts with the less activated alkyne methyl propionate (R = H, R' = CO₂CH₃) but at a very much slower rate than with the diester DMAD [13]. More recently, the relatively electron-rich isocyanide complexes Fe(α -diimine)(CO)_{3-n}(CNR)_n have even been found to undergo cycloaddition with the activated alkene, dimethyl maleate [14]. However, the PAP complexes of types **7** and **8** do not react with either the monoester alkyne methyl butynoate (R = CH₃, R' = CO₂CH₃) or with dimethyl maleate. These observations illustrate further the importance of the electronic character of both reactants in the cycloaddition reaction.

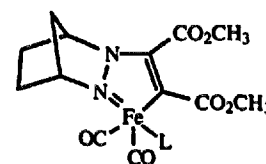
As stated earlier, the reaction of **8a** and **8c** with DMAD in THF gave a mixture of products. In addition to the carbonyl stretching bands due to **11a** or **11c**, additional bands appear at about 2057 and 1980 cm⁻¹ with a shoulder at about 1990 cm⁻¹ on the second band; this pattern is indicative of a tricarbonyl species. We believe these bands arise from a reaction using the CO released through partial decomposition of **11a** or **11c**. When the reaction of **8** (or **9**) with DMAD is carried out in an atmosphere of CO, **11** (or **12**) is not observed and only the bands of the tricarbonyl product grow. A solution of **11** (or **12**) shows no change under a CO atmosphere, but if uncoordinated DMAD is also present, as is the case in the reaction mixture beginning with **8** (or **9**), the conversion to the new species occurs slowly over several days. However, this reaction with **11** (or **12**) is much too slow to account for the formation of the new species starting from **8** (or **9**). Consequently, it must arise from **8** (or **9**) in a process that occurs prior to the formation of **11** (or **12**). Proton NMR of the crude solids left after solvent removal indicates that the material is a mixture whose composition varies from one synthesis to another. Signals due to coordinated PAP and to the two DMAD ester groups, which are inequivalent, are always present, but signals due to PⁿBu₃ or P(OCH₃)₃ are absent. Unfortunately, repeated attempts

to isolate this new, low-yield species in pure form have failed.

Compounds with the 2,3,1-diazaferrole ring structure similar to **11** and **12** have been reported previously. The reaction of an alkyne with Fe₂(CO)₆L, where L is a cyclic diazene, provides complexes of type **13**, which arise from the insertion of the alkyne into an Fe–N bond followed by loss of an Fe(CO)₃ group [15]. The crystal structure of the tricarbonyl **14a** has been determined [16]. Under electrochemically reducing conditions, one of the CO groups in **14a** can be replaced by P(OCH₃)₃ or PPh₃ to give **14b** or **14c** respectively, which have only been characterized spectroscopically in solution [17]. The isolation of **14a** suggests that the tricarbonyl analog of **11** or **12** should be stable if it is formed. Indeed, it is possible that the tricarbonyl compound(s) we observe when **8a-c** or **9b** react with DMAD in the presence of CO includes this complex since the carbonyl stretching frequencies are comparable with those reported for **14a** [15,17].



13



14a: L = CO

14b: L = P(OCH₃)₃14c: L = PPh₃

3.2. Spectroscopy

The infrared spectra of complexes **11a-c** and **12b** exhibit two metal–carbonyl stretching bands of about equal intensity. The frequencies are essentially identical for **11a-c**, which is consistent with the pyridyl group not being coordinated to the iron. When the pyridyl group of the PAP ligand is coordinated to the iron atom, as in **7** [7] and **8**, the carbonyl frequencies are sensitive to the substituents on the pyridyl ring.

It is noteworthy that the carbonyl stretching frequencies for **14b** are reported at 1990 and 1875 cm⁻¹ in CHCl₃, while those for **12b** are at 2008 and 1952 cm⁻¹ in this solvent. The difference in frequency of the second band is surprisingly large and may reflect significant differences in the geometry around the iron atom in the two compounds.

The ¹H NMR spectra of all the complexes synthesized in this study were readily assigned based on proton–proton coupling analysis and by analogy with the uncoordinated ligands. The spectra of **11a-c** and **12b** all show that the ester methyl groups are magnetically inequivalent.

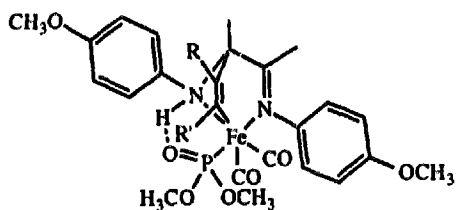
Table 4
Electronic absorption spectral data (nm) for the DMAD cycloaddition products

Compound	$\lambda_{\max}(\epsilon)^a$	
	Hexanes	Methanol
11a	520 (3930), 388 (5480), ~ 320 (10400)	514 (3570), ~ 390 (5350), 322 (11100)
11b	524 (4500), 390 (5810), ~ 320 (11400)	516 (4140), 392 (5640), 326 (11200)
11c	526, 392, ~ 320 sh ^b	508 (3200), ~ 390 (4370), ~ 320 (10300)
12b	494, 368, ~ 300 sh ^b	486 (4570), ~ 375 (5420)

^a Resolution ± 2 nm. For features without clear maxima, ϵ is given at the wavelength cited.

^b Relatively insoluble; recorded from a saturated solution.

The ¹³C NMR spectral assignments of the ligands **6a–d** were facilitated by noting the effects of the different substituents on the chemical shifts and, in some cases, by analysis of fully coupled spectra. Similar considerations, as well as analogy with the uncoordinated ligands, guided the assignments of the complexes **8a–d**, **9b**, **11a–c**, and **12b**. Unfortunately, the ¹³C NMR spectra of **14a–c** or of the complexes of type **13** are not available to assist in the assignments of **11a–c** and **12b**; only the carbonyl carbon resonances of **14a–c** have been reported [17]. In **11a–c** and **12b** the greatest difficulty was encountered in the assignment of the quaternary carbons originating from DMAD. In the fully coupled spectrum of **11b** the signals at 177.6 and 162.3 ppm become quartets and are assigned to the carbonyl carbons of the ester groups, with the higher chemical shift being associated with the one closer to the iron atom. These shifts are very similar to those in an α -diimine complex **15** ($R = R' = \text{CO}_2\text{CH}_3$), which is closely related to a type **2** complex [1]. The peak at 141.2 ppm and the doublet at 172.8 ppm arising from coupling to phosphorus in **11b** show no coupling to protons and are assigned to the carbon atoms in the diazaferrole ring. The coupling to phosphorus and the larger downfield shift lead us to assign the doublet at 172.8 ppm to the carbon bonded to iron. In the bicyclic structure **15** this carbon signal appears at around 220 ppm with $^3J_{\text{C-P}} > 30$ Hz, while the more distant olefinic carbon signal is at 131.8 ppm with $^3J_{\text{C-P}} = 3.8$ Hz. The chemical shift of the DMAD carbon bonded to iron in structures of type **11** and **12** compared with type **2** may be the most diagnostic feature for distinguishing between structures in which the iron is part of a single ring or in a bicyclic complex. It would be of interest to have examples of both structural types for either the α -diimine or the PAP case to test this idea.



15

Compounds **11a–c** are red in solution while **12b** is orange-red. Their UV–visible spectral features are summarized in Table 4. The peak maxima are relatively insensitive to increasing methyl substitution on the pyridyl ring in **11a–c**. The intensity of the band in the visible region is consistent with an MLCT transition, but if this is the origin, the relative insensitivity to solvent effects would require similar molecular polarity in the ground and excited states [18].

3.3. Structure

The molecular structure of **12b** has been determined by single-crystal X-ray diffraction, and a computer-generated drawing is shown in Fig. 1. The structure is similar to that of **14a** [16] and represents only the second determination of a compound with a 2,3,1-diazaferrole ring. The structure of **12b** may be described as a distorted square pyramid, in which the trimethylphosphite group occupies the apical position. This description is analogous to that of **14a** [16]. An alterna-

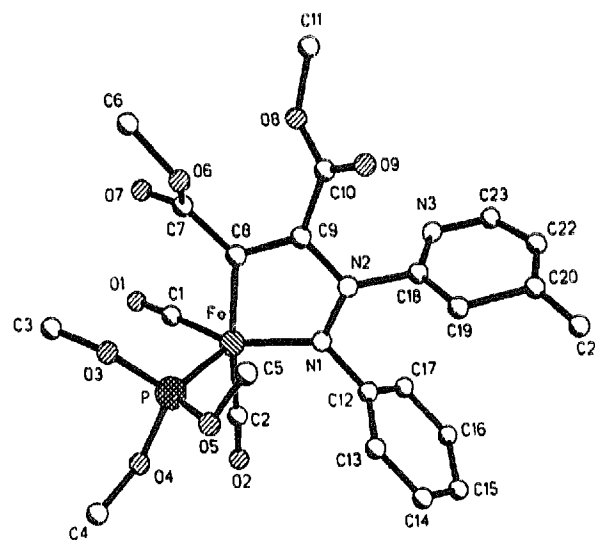
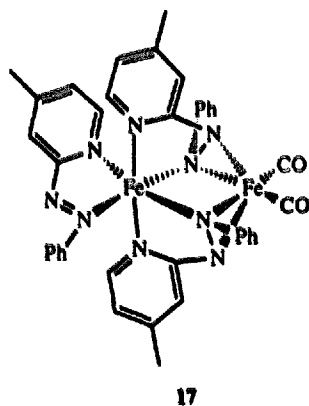
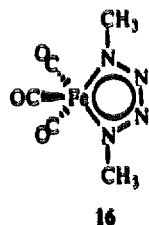


Fig. 1. Computer-generated drawing of $\text{Fe}(\text{CO})_2(\text{P}(\text{OCH}_3)_3)-(\text{C}(\text{COOCH}_3)=\text{C}(\text{COOCH}_3)\text{N}(4\text{-CH}_3\text{-2-py})\text{N}(\text{Ph}))$ (**12b**). Hydrogen atoms have been omitted for clarity.

tive description of **12b** is that of a distorted trigonal bipyramid with C(2) and C(8) in the axial positions. The much smaller P–Fe–N(1) angle of **12b** relative to the comparable angle in **14a** may be a consequence of nitrogen also being part of the norbornene bicyclic system in **14a**.

As with **14a**, the diazaferrole ring in **12b** is essentially planar. None of the ring atoms lies more than 0.02 Å off the best least-squares plane, and the largest dihedral angle is only 3.1°. The bond lengths in the ring are comparable with those in **14a** and are consistent with the proposal that this is a delocalized π system [16,19]. Additional support for a π component in the iron–nitrogen bond comes from comparisons with structures **16** and **17**. At 1.853(8) Å the Fe–N(1) bond is similar in length to the value of 1.83 ± 0.03 Å for the Fe–N bonds in the tetraazaferrole complex $(\text{CO})_3\text{Fe}(\text{N}_4(\text{CH}_3)_2)$ **16** [20], for which theoretical and experimental studies support a delocalized π system [21]. In the PAP bridged dimer **17** the Fe–N_{azo} bond of the non-bridging **6b** ligand, which includes a π component, is 1.856(6) Å, while the Fe–N_{azo} bonds for the bridging **6b** ligands, in which there is no π bonding, average 1.98 Å [7]. The orientations of the groups attached to the carbon or nitrogen atoms of the diazaferrole ring in **12b** indicate that none are conjugated with the ring.



The presence of delocalized π bonding in the diazaferrole ring of **11** or **12** may account for the difference in the reaction sequences of the α -diimine and PAP systems after the initial cycloaddition step to give a bicyclic intermediate (**2** or **10**). A single five-membered ring structure such as **11** accompanied by π donation to the iron from nitrogen is possible for either ligand and would satisfy the 18-electron rule. However, only the 2,3,1-diazaferrole structure derived from PAP has the possibility of π delocalization in the ferrole ring; π

delocalization is precluded in the 2-azaferrole structure that arises from an α -diimine because an sp^3 hybridized carbon replaces the sp^2 hybridized nitrogen not bonded to iron. Without the additional stabilization of delocalized π bonding, the azaferrole would not be favored over the bicyclic structure.

4. Supplementary material available

Tables of bond angles and bond lengths, anisotropic displacement coordinates, hydrogen atom coordinates, and structure factors (20 pages) for **12b** are available from the authors.

Acknowledgements

We gratefully acknowledge the donors of the Petroleum Research Fund, administered by the American Chemical Society, for financial support. ALC, FVM, and MJT thank the Merck Company Foundation for summer support through a grant to Oberlin College.

References and notes

- [1] H.-W. Fröhlich, F. Seils and C.H. Stam, *Organometallics*, **8** (1989) 2338.
- [2] M. van Wijnkoop, P.P.M. de Lange, H.-W. Fröhlich and K. Vrieze, *Organometallics*, **11** (1992) 3607.
- [3] P.P.M. de Lange, H.-W. Fröhlich, M. van Wijnkoop, K. Vrieze, Y. Wang, D. Heijdenrijk and C.H. Stam, *Organometallics*, **9** (1990) 1691.
- [4] P.P.M. de Lange, H.-W. Fröhlich, M.J.A. Kraakman, M. van Wijnkoop, M. Kranenburg, A.H.J.P. Groot, K. Vrieze, J. Fraanje, Y. Wang and M. Numan, *Organometallics*, **12** (1993) 417.
- [5] P.P.M. de Lange, M. van Wijnkoop, H.-W. Fröhlich, K. Vrieze and K. Goubitz, *Organometallics*, **12** (1993) 428.
- [6] M.N. Ackermann, C.R. Barton, C.J. Deodene, E.M. Specht, S.C. Keill, W.E. Schreiber and H. Kim, *Inorg. Chem.*, **28** (1989) 397.
- [7] M.N. Ackermann, J.W. Naylor, E.J. Smith, G.A. Mines, N.S. Amin, M.L. Kerns and C. Woods, *Organometallics*, **11** (1992) 1919.
- [8] G.M. Sheldrick, *SHELXTL PLUS*, Vers. 4.1, Siemens Analytical X-ray Instruments, Madison, WI, 1990.
- [9] Neutral-atom scattering factors and corrections for anomalous scattering were taken from: D.T. Cromer and J.T. Waber, *International Tables for X-ray Crystallography*, Vol. IV, Kynoch Press, Birmingham, UK, 1974.
- [10] R.H. Crabtree, *The Organometallic Chemistry of the Transition Metals*, Wiley-Interscience, New York, 2nd edn., 1994.
- [11] C.A. Tolman, *Chem. Rev.*, **77** (1977) 313.
- [12] H.-Y. Liu, K. Eriks, A. Prock and W.P. Giering, *Organometallics*, **9** (1990) 1758.
- [13] H.-W. Fröhlich and F. Seils, *J. Organomet. Chem.*, **323** (1987) 67.
- [14] P.P.M. de Lange, R.P. de Boer, M. van Wijnkoop, J.M. Ernst-

- ing, H.-W. Frühauf, K. Vrieze, W.J.J. Smeets, A.L. Spek and K. Goubitz, *Organometallics*, **12** (1993) 440.
- [15] A. Albin and H. Kisch, *J. Organomet. Chem.*, **101** (1975) 231.
- [16] R. Battaglia, C.C. Frazier III, H. Kisch and C. Krüger, *Z. Naturforsch., Teil B*, **38** (1983) 648.
- [17] F.R. Estevan, P. Lahuerta and J. Latorre, *Inorg. Chim. Acta*, **116** (1986) L33.
- [18] W. Kaim, S. Kohlmann, S. Ernst, B. Olbrich-Deussner, C. Ressenbacher and A. Schulz, *J. Organomet. Chem.*, **321** (1987) 215.
- [19] H. Kisch and P. Holzmeier, *Adv. Organomet. Chem.*, **34** (1992) 67.
- [20] R.J. Doedens, *J. Chem. Soc., Chem. Commun.*, (1968) 1271.
- [21] W.C. Trogler, C.E. Johnson and D.E. Ellis, *Inorg. Chem.*, **20** (1981) 980.